AD-A121 087 NUMERICAL SIMULATION OF A POSSIBLE FREEZING AND SHEET FORMATION MECHANISM..(U) NAVAL RESEARCH LAB WASHINGTON DC S T ZALESAK ET AL. 25 OCT 82 NRL-MR-4919 1/1

UNCLASSIFIED MIPR-82-504 F/G 12/1 NL

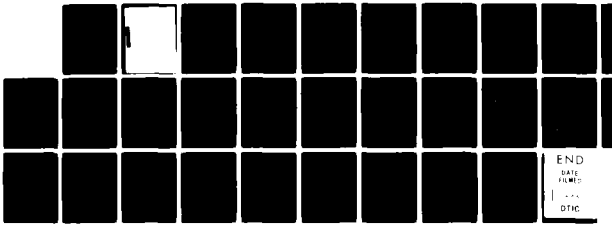

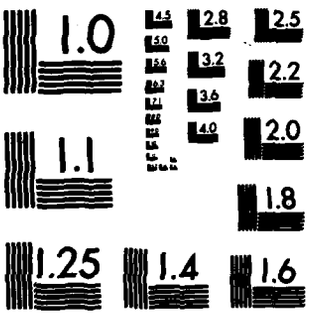

SECURITY CLASSIFICATION OF THIS PAGE (When Data Entered)

REPORT DOCUMENTATION PAGE	READ INSTRUCTIONS BEFORE COMPLETING FORM
1. REPORT NUMBER: NRL Memorandum Report 4919 — 2. GOVT ACCESSION NO.: A121087	3. RECIPIENT'S CATALOG NUMBER:
4. TITLE (and Subtitle): NUMERICAL SIMULATION OF A POSSIBLE FREEZING AND SHEET FORMATION MECHANISM FOR BARIUM CLOUD STRIATIONS	5. TYPE OF REPORT & PERIOD COVERED: Interim report on a continuing NRL problem.
	6. PERFORMING ORG. REPORT NUMBER:
7. AUTHOR(s): S.T. Zalesak, J.A. Fedder, and S.L. Ossakow	8. CONTRACT OR GRANT NUMBER(s):
9. PERFORMING ORGANIZATION NAME AND ADDRESS: Naval Research Laboratory, Washington, DC 20375	10. PROGRAM ELEMENT, PROJECT, TASK AREA & WORK UNIT NUMBERS: 62715H; 47-0889-0-2
11. CONTROLLING OFFICE NAME AND ADDRESS: Defense Nuclear Agency, Washington, DC 20305	12. REPORT DATE: October 25, 1982
	13. NUMBER OF PAGES: 35
14. MONITORING AGENCY NAME & ADDRESS(if different from Controlling Office)	15. SECURITY CLASS. (of this report): UNCLASSIFIED
	15a. DECLASSIFICATION/DOWNGRADING SCHEDULE:

16. DISTRIBUTION STATEMENT (of this Report)

Approved for public release; distribuiton unlimited.

17. DISTRIBUTION STATEMENT (of the abstract entered in Block 20, if different from Report)

18. SUPPLEMENTARY NOTES

This research was sponsored by the Defense Nuclear Agency under Subtask S99QAXHC, work unit 00032, and work unit title "Plasma Structure Evolution" with funds provided under MIPR 82-504.

19. KEY WORDS (Continue on reverse side if necessary and identify by block number)

Computer simulation
Numerical simulation
Barium clouds
Ionospheric plasma clouds
Gradient drift instability
Plasma clouds

PRESENTED 15

20. ABSTRACT (Continue on reverse side if necessary and identify by block number)

We present a possible mechanism for the "freezing," or apparent freezing, of barium cloud striations and for the formation of long thin sheets of barium on the leading edge of the cloud. The essence of the model is that the finite Pedersen mobility of the barium ions allows them to separate from the electron cloud. The barium is replaced in the electron cloud by the ions constituting the ambient ionosphere, which are compressed up

(Continues)

DD FORM 1 JAN 73 1473 EDITION OF 1 NOV 65 IS OBSOLETE
S/N 0102-014-6601

SECURITY CLASSIFICATION OF THIS PAGE (When Data Entered)

20. ABSTRACT (Continued)

to the required densities by their own Pederseh mobility. In the process of existing the electron cloud, the barium is expanded and hence attains a density lower than when it coexisted with the electron cloud. For many ionospheric parameters the barium will have in effect left the region of further structuring, which will still be proceeding the electron cloud. As the barium leaves the electron cloud, it forms a long thin sheet of lower density barium, one side of which is considerably steeper than the other, which extends from the leading (nonstructuring) edge of the cloud. An observer watching only the barium would conclude that the cloud had frozen. Further, the electron cloud itself may decay if the ions coexisting with it are subject to a fast recombination chemistry.

CONTENTS

1. Introduction 1

2. Theory.....2

3. The Pedersen Leakage Mechanism: The Simplest case.....5

4. The Pedersen Leakage Mechanism: More General Ionospheric Parameters....13

5. Numerical Simulations.....15

6. Conclusions and Future Work.....19

Acknowledgment 21

References.....21

NUMERICAL SIMULATION OF A POSSIBLE FREEZING AND SHEET FORMATION MECHANISM FOR BARIUM CLOUD STRIATIONS

1. Introduction

Although many features of barium cloud striations are understood (Ossakow 1979; Ossakow et al., 1982), there exist several aspects of the phenomenology which as of yet lack a satisfactory explanation. This paper addresses two of these phenomena: 1) the persistence of striations with scale sizes in the kilometer range for times on the order of hours [Prettie et al., 1977, J.A. Fedder and W. Chestnut, private communication, 1980]; and 2) the formation and persistence of long thin "sheets" of barium on the leading (non-structuring) side of the cloud. In what follows we shall attempt to show that both of these phenomena can be explained by a proper understanding of the role played by the finite Pedersen mobility both of the barium ions and of the ions constituting the ambient ionosphere. In essence we find that the finite Pedersen mobility of the ions vis a vis the electrons, which essentially have no Pedersen mobility at all, allows the barium to "leak" out of the electron cloud. Quasineutrality in the electron cloud is maintained by incoming ambient ionosphere ions (denoted here by O^+, but these could also be NO^+ or other ionspheric ion constituents), which compress up to the electron density as they replace the barium in the cloud. For many ionospheric parameters, once the barium has left the electron cloud, it is essentially free of the polarization fields associated with the electron cloud and hence immune to further structuring. An observer watching only the barium might conclude that it had "frozen". Further, the electron cloud itself may decay if the ions coexisting with it are subject to fast recombination chemistry.

The above ideas were arrived at independently by Prettie [1981] and by Fedder (private communication, 1981). The conclusions of the present paper differ from those in Prettie [1981] primarily in the fact that we find that the formation of sheets is directly related to the leaking of barium from the electron cloud, as just discussed, and is totally unrelated to the formation of "quadrupole" potential fields, as postulated by Prettie [1981]. Rather, the sheet forms as the barium leaks out of one side of the electron cloud. In the process it also leaves the regions of shielding provided by the enhanced Pedersen conductivity associated with the enhanced electron density (for many ionospheric parameters), and over a fairly short distance enters the unshielded region where it takes on the ambient $c\,\underline{E}_o \times \underline{B}/B^2$ drift velocity. From the reference frame of the center of the electron cloud, we are slowly

Manuscript submitted August 5, 1982.

injecting barium into a flow field transverse to the injection direction which starts at zero at the electron cloud center and rapidly becomes large over a very short distance at the "edge" of the electron cloud. The result is a long, low density string of barium which we perceive as a "sheet". This concept, as well as the meaning of the term "many ionospheric parameters" used above, will be given in more detail later in this paper.

In section 2 of this paper we briefly review the theory and relevant equations for the multilevel/multispecies ionospheric barium cloud problem. In section 3 we describe in more detail the basic Pedersen drift mechanism proposed by Prettie [1981] and by Fedder (private communication 1981), and also present our proposed mechanism for barium sheet formation. In section 4 we discuss the effect of the Pedersen drift mechanism under various ionospheric parameter regimes within the context of a two level (two species) model. In section 5 we present preliminary numerical simulation results which seem to bear out the analysis, although one aspect of the simulations, the steep density gradients on one side of the sheet, is not well understood by us at this time. Finally in section 6 we present our conclusions and plans for future work.

2. Theory

Consider a fluid plasma species α imbedded in a neutral gas and a magnetic field $\underline{B}$, which we assume is aligned along the cartesian axis $\hat{z}$. Under the time scales and ionospheric parameters of interest for the ionospheric barium cloud striations problem, this plasma will respond to an external force perpendicular to the magnetic field, $\underline{F}_{\alpha\perp}$, in two ways: 1) by drifting in the direction of the external force (Pedersen mobility); and 2) by drifting in a direction perpendicular to both the external force and to the magnetic field (Hall mobility). Specifically, if the momentum equation for species α is

$$\left(\frac{\partial}{\partial t} + \underline{v}_\alpha \cdot \underline{\nabla}\right)\underline{v}_\alpha = \frac{q_\alpha}{m_\alpha}\left(\underline{E} + \frac{\underline{v}_\alpha \times \underline{B}}{c}\right) - \nu_{\alpha n}\left(\underline{v}_\alpha - \underline{U}_n\right) + \frac{1}{m_\alpha}\underline{G}_\alpha \qquad (2.1)$$

and we define the external force to be

$$\underline{F}_\alpha \equiv q_\alpha \underline{E} + \nu_{\alpha n} m_\alpha \underline{U}_n + \underline{G}_\alpha \qquad (2.2)$$

then

$$\underline{v}_{\alpha\perp} = k_{1\alpha}\underline{F}_{\alpha\perp} + k_{2\alpha}\underline{F}_{\alpha\perp} \times \hat{z} \tag{2.3}$$

where

$$k_{1\alpha} = \frac{\nu_{\alpha n}}{\Omega_\alpha}\frac{c}{|q_\alpha B|}\left[1 - \frac{(\nu_{\alpha n}/\Omega_\alpha)^2}{1 + (\nu_{\alpha n}/\Omega_\alpha)^2}\right] \tag{2.4}$$

$$k_{2\alpha} = \frac{c}{q_\alpha B}\left[1 - \frac{(\nu_{\alpha n}/\Omega_\alpha)^2}{1 + (\nu_{\alpha n}/\Omega_\alpha)^2}\right] \tag{2.5}$$

Here we have neglected the left hand side of (2.1) since we are interested only in average drift velocities over time scales that are long compared to either the mean time between collisions or the gyroperiod. Also we have ignored all collisions except those between species α and the neutral gas. The notation in the above equations is as follows: $\underline{v}_\alpha$, q_α and m_α are the fluid velocity, charge per particle, and mass per particle respectively of species α; $\underline{E}$ is the electric field, t is time, c is the speed of light, $\nu_{\alpha n}$ is the collision frequency of species α with the neutral gas, $\underline{U}_n$ is the neutral gas velocity, Ω_α is the cyclotron frequency of species α, $\Omega_\alpha \equiv |q_\alpha B/(m_\alpha c)|$, and G_α is a term meant to represent all of the other external forces on species α (gravity, pressure gradients, etc). The subscript $\perp$ refers to the components of the respective vector which are perpendicular to $\underline{B}$.

Starting with the above, one can derive the set of partial differential equations describing the barium cloud striations problem by demanding that each species α obey a continuity equation and that $\nabla\cdot\underline{j} = 0$ where $\underline{j}$ is the electric current, which is to say that we demand electrical quasi-neutrality globally for all time. The quantity $\underline{j}$ is defined by multiplying (2.3) by $q_\alpha n_\alpha$, where n_α is the number density of species α, and summing over α. If one further assumes that $\underline{E} = -\nabla\phi$ where ϕ is the scalar electrostatic potential, then $\nabla\cdot\underline{j} = 0$ yields an elliptic equation for ϕ. This derivation is given in several papers [Lloyd and Haerendel, 1973; Goldman et al., 1974; Perkins et al., 1973 for example] and will not be reproduced here. Rather, we simply describe the other simplifying assumptions and give the final equations.

We find that for ionospheric barium clouds it is a very good approximation to assume that the electrostatic potential ϕ is constant along magnetic field lines, i.e. $\phi = \phi(x,y)$ where the magnetic field $\underline{B}$ is aligned along $\hat{z}$ in an x-y-z cartesian coordinate system. Further we find that since the currents parallel to $\underline{B}$ are carried primarily by electrons and since the motion of ions parallel to $\underline{B}$ consists primarily of a slow diffusion plus a bulk "falling" of the cloud, since $\underline{g}\cdot\underline{B} \neq 0$ where $\underline{g}$ is the gravitational acceleration, it is sufficient to represent the ions as an array of two-dimensional planes of plasma perpendicular to $\underline{B}$, each moving with the bulk "falling" velocity along $\underline{B}$, and hence to treat numerically only the transport of ions perpendicular to $\underline{B}$ within each layer. For cases where multiple ion species coexist in one layer, this layer is simply treated as multiple layers with the same location in space. This treatment is consistent with our neglect of all collisions except ions with neutrals and electrons with neutrals. Thus we use the phrase "multilevel/multispecies" to describe the model.

We draw the readers attention to the following remarks, whose importance shall become clear as we progress. The right hand side of (2.3) gives explicitly the Pedersen and Hall components, respectively, of the drift velocity of species α. Looking at (2.4) we find that $k_{1\alpha} \approx 0$ for electrons, since $\nu_{en}/\Omega_e \approx 0$ (where the subscript e denotes electrons). Thus ions, for which $\nu_{\alpha n}/\Omega_\alpha$ ranges from 0.01 to greater than 1.0, are endowed with a Pedersen mobility which is lacking for the electrons: ions and electrons do not move together. Equally important, under the conditions that $\underline{B}$ is uniform and that the external force $\underline{F}_{\alpha\perp}$ can be written as the gradient of a scalar, conditions which are satisfied in most of the barium cloud problems we shall consider, the Hall component of $\underline{v}_{\alpha\perp}$ is divergence free while the Pedersen component is not. Thus individual fluid elements of ions may compress or expand, while the electron fluid satisfies the constraint of incompressibility (in the x-y plane).

In this paper we shall limit our discussion to a model consisting of only two layers or species of ions, as this will considerably simplify the understanding of the ideas we shall put forth without, we believe, compromising the ideas themselves. We shall also confine our external force to an externally imposed electric field $\underline{E}_o$ which is perpendicular to $\underline{B}$, i.e.,

$\underline{E}_o = E_{ox}\hat{x} + E_{oy}\hat{y}$. We denote by n_1 and n_2 the integrated (along $\underline{B}$) number density of the ions (and by quasi-neutrality, the electrons) in levels 1 and 2 respectively. The equations describing this system are then

$$\partial n_\alpha/\partial t + \nabla_\perp\cdot(n_\alpha \underline{v}_{\alpha\perp}) = 0 \qquad \alpha = 1,2 \tag{2.6}$$

$$\nabla_\perp\cdot[(\Sigma_{p1} + \Sigma_{p2})\nabla_\perp\phi] + H = \underline{E}_o\cdot\nabla_\perp(\Sigma_{p1} + \Sigma_{p2}] \tag{2.7}$$

$$H \equiv -\frac{\partial}{\partial x}\left[(\Sigma_{h1} + \Sigma_{h2})\left(\frac{\partial\phi}{\partial y} - E_{oy}\right)\right] + \frac{\partial}{\partial y}\left[(\Sigma_{h1} + \Sigma_{h2})\left(\frac{\partial\phi}{\partial x} - E_{ox}\right)\right] \tag{2.8}$$

$$\Sigma_{p\alpha} \equiv \frac{\nu_{\alpha n}}{\Omega_\alpha}\left(1 + (\nu_{\alpha n}/\Omega_\alpha)^2\right)^{-1} n_\alpha c\, q_\alpha/|B|, \ \alpha = 1,2 \tag{2.9}$$

$$\Sigma_{h\alpha} \equiv \frac{\nu_{\alpha n}}{\Omega_\alpha}\Sigma_{p\alpha}, \qquad \alpha = 1,2 \tag{2.10}$$

The terms comprising H in (2.7) are referred to as the "Hall terms", and for the purposes of the ideas to be presented in the present paper can be considered to be small. The quantity $\underline{v}_{\alpha\perp}$ in (2.6) is defined by (2.3)-(2.5) where

$$\underline{F}_{\alpha\perp} = q_\alpha(\underline{E}_o - \nabla\phi) \tag{2.11}$$

3. The Pedersen Leakage Mechanism: The Simplest Case

As mentioned in the previous section we shall consider only a model consisting of two ion species. Since we are neglecting all collisions except those between ions and neutrals (recall we have set $\nu_{en}/\Omega_e \approx 0$), and since we are assuming that the only external forces acting are electric fields perpendicular to $\underline{B}$, which are constant along any given magnetic field line, one can conceptually think of these layers of plasma as coexisting at the same plane in space, as long as we enforce the caveat that the two ion species α may "see" different neutral densities, which will be reflected in the value of $\nu_{\alpha n}$. Hence all of our diagrams of the physical processes can be

of a single two-dimensional plane.

Furthermore, we shall specifically take the two ion species to be Ba^+ and the ambient ionosphere ion O^+, with the understanding that by "O^+" we might also mean NO^+ or any of the other ambient ionospheric ions. Thus we shall henceforth use the subscripts b and o to denote Ba^+ and O^+, rather than the subscripts 1 and 2 used previously. Within the context of this model, it is clear that

$$n_b + n_o = n_e \tag{3.1}$$

where n_e denotes the integrated electron density. Hence one can substitute a continuity equation for n_e

$$\partial n_e/\partial t + \nabla_\perp \cdot (n_e v_{e\perp}) = 0 \tag{3.2}$$

for one of the two equations in (2.6), since the substituted density can always be recovered from (3.1). For the remainder of this paper we shall use this fact and display profiles of barium density and electron density. For the purposes of this section only, we impose one last assumption:

$$\nu_{bn}/\Omega_b = \nu_{on}/\Omega_o \tag{3.3}$$

Thus the two ion species are identical in terms of their electrical properties vis à vis (2.7) and in terms of their response to an external force (2.3). In fact, if we were interested only in electron densities and not in the actual identities of the ion species making up the "electron cloud", it would suffice to sum the two ion layers and treat them as simply one layer. This is precisely the implicit assumption made in the "one level model" [McDonald et al., 1980]. Instead we shall choose to follow each ion species separately, as this will have interesting consequences.

In Fig. 1 we show a simplified picture of an ionized barium cloud which has been placed in a uniform ionosphere consisting of O^+ ions. Isodensity contours of electrons are shown as solid lines, while those for barium are shown as dashed lines. At $t = 0$ the two sets of contours are identical. We impose an ambient electric field $\underline{E}_o$ directed to the right. The

electron/barium cloud will partially shield itself from this field, and experience an average reduced field E′, still directed to the right in Fig. 1. Referring to (2.3)-(2.5) and recalling that $\nu_{en}/\Omega_e \approx 0$ we find that the electron cloud simply drifts downward at velocity cE′/B. If we assume that ν_{bn}/Ω_b is $\sim 10^{-2}$, then we see that the barium cloud too drifts downward at a velocity very close to cE′/B. However the barium also experiences a Pedersen drift to the right of value approximately (ν_{bn}/Ω_b) cE′/B. If the clouds initially have diameter D and remain undeformed the barium cloud will completely exit the electron cloud in a time $t = (\Omega_b/\nu_{bn})DB/(cE')$, as depicted on the left side of Fig. 1. Of course by quasi-neutrality the ions in the electron cloud would then consist of 0^+ ions which had been compressed up to the required density (the electron density) as they entered the electron cloud from the left. By the same principle, the barium must expand as it leaves the electron cloud to the right, showing that this motion cannot truly take place without deformation. Also one might expect to see the normal electron cloud steepening and structuring during this time interval. In addition as the barium exits the electron cloud to the right it leaves a region where the electric field has been reduced by shielding to E′ and enters a region where E takes on the larger value E_o. Accordingly as it leaves it gets caught up in this higher velocity field and forms a sheet of lower density barium which leads the cloud. This somewhat more realistic picture is depicted on the right side of Fig. 1.

The above picture describes in qualitative terms the essence of this paper. We will now expand upon this idea in more quantitative terms by simplifying the picture even further so that quantitative results can be obtained and that a more precise picture may be obtained of the compression and expansion processes proceeding in the ion fluids.

In Fig. 2a we again show a profile, n_α vs x, of an ionized barium cloud which has been placed in a uniform ionosphere consisting of 0^+ ions, again subject to an externally imposed electric field $\underline{E}_o$ pointing to the right. This time, however, we choose the cloud and ionosphere to be infinite in the y direction, the so-called slab geometry. We denote the cloud thickness by L and assume for the sake of example that its integrated density is exactly twice that of the background 0^+ ionosphere. The barium fluid is shown cross-hatched, while the 0^+ fluid is shown without cross-hatching. Again we are

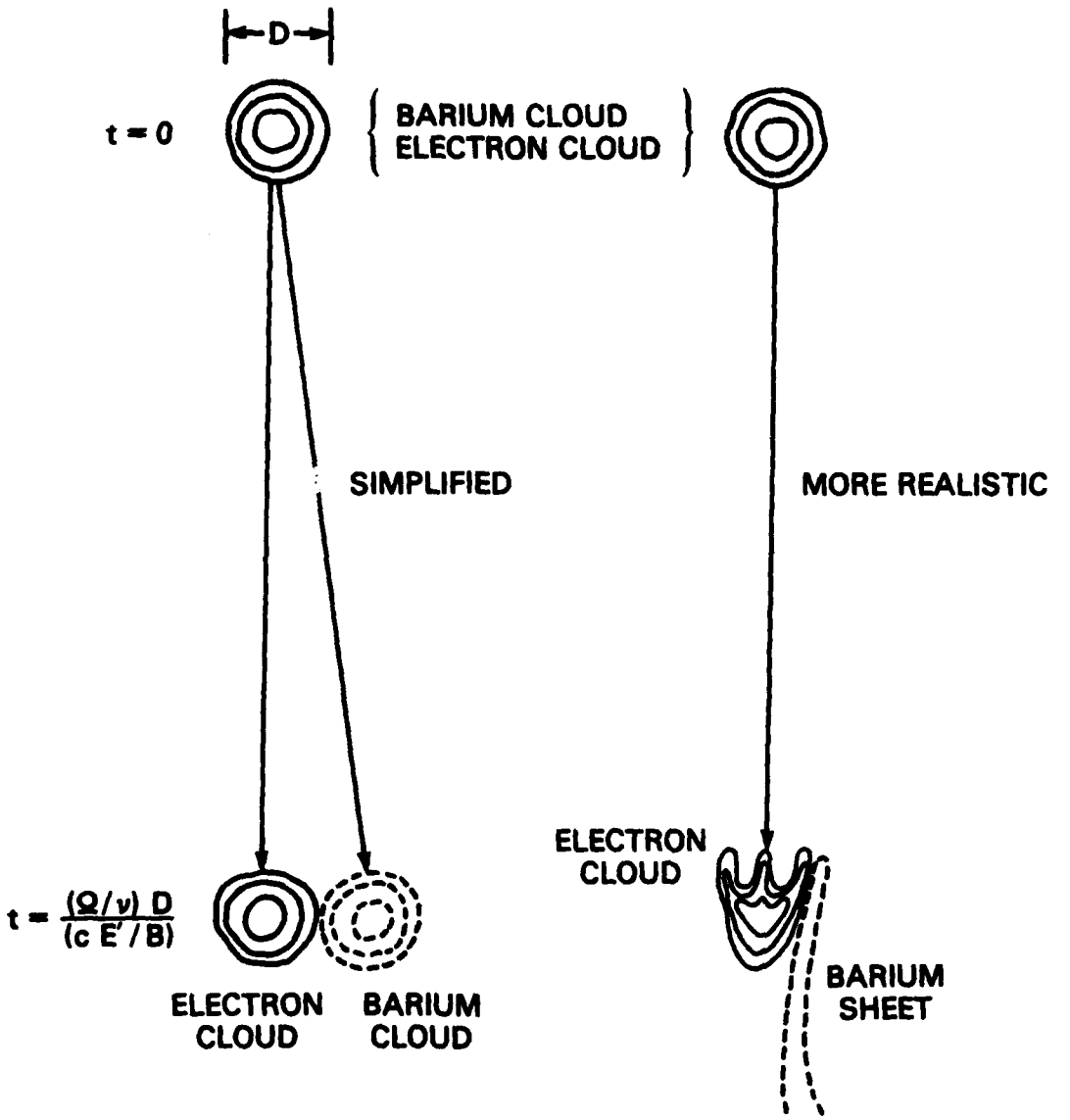

Fig. 1 — Schematic depiction of the evolution of an ionized barium cloud subject to an externally imposed rightward directed electric field E_0. The cloud will partially shield itself, yielding a net field E' inside the cloud. Rightward Pedersen drifts then allow the barium to separate from the electron cloud in a time t_0. A simplified picture is shown on the left, while a more realistic evolution is depicted on the right.

assuming that $\nu_{bn}/\Omega_b = \nu_{on}/\Omega_o$ and that both quantities are $\sim 10^{-2}$. Then the potential equation (2.7) has the simple solution

$$\begin{aligned} E &= E_o \quad \text{outside the electron cloud} \\ &= E_o/3 \quad \text{inside the electron cloud} \end{aligned} \tag{3.4}$$

If $\underline{B}$ is taken to be upward in Fig. 2 then both ion species and the electrons are all drifting toward the reader with velocity very close to cE/B. However both the ions have in addition a Pedersen drift to the right given by

$$v_p = (\nu_{bn}/\Omega_b)cE/B \tag{3.5}$$

where v_p is the rightward Pedersen velocity in this example. Noting the discontinuous changes in E that occur at the edges of the electron cloud, we see that ion compression is taking place at the left edge of the electron cloud while expansion is taking place at the right edge. In fact in this example, the ions experience a compression of exactly a factor of 3 as they cross the left edge of the electron cloud, and an expansion of exactly a factor of 3 as they exit the right edge. Of course this is exactly what is required by the condition of quasi-neutrality ($\underline{\nabla} \cdot \underline{j} = 0$). One can also calculate the time t_o it takes for the barium to completely exit the electron cloud in a manner analogous to that used previously for Fig. 1. One obtains

$$t_o = \frac{L}{\left(\frac{\nu_{bn}}{\Omega_b}\right)\frac{cE_o}{3B}} \tag{3.6}$$

where L is the width of the cloud. In Fig. 2b we show the time evolution of the profile depicted in Fig. 2a for various units of time in terms of t_o. Note that after time t_o: 1) the "cloud" consists totally of O^+ ions; 2) the barium extends over a region three times its original extent but down by a factor of three in density; 3) the barium is completely removed from gradients in n_e and hence Σ_p and therefore would be removed from any further structuring taking place in the analogous situation for a two-dimensional cloud, as in Fig. 1. It is postulated that this may very well be what is known as "freezing". It should also be noted that if the O^+ cloud is subject

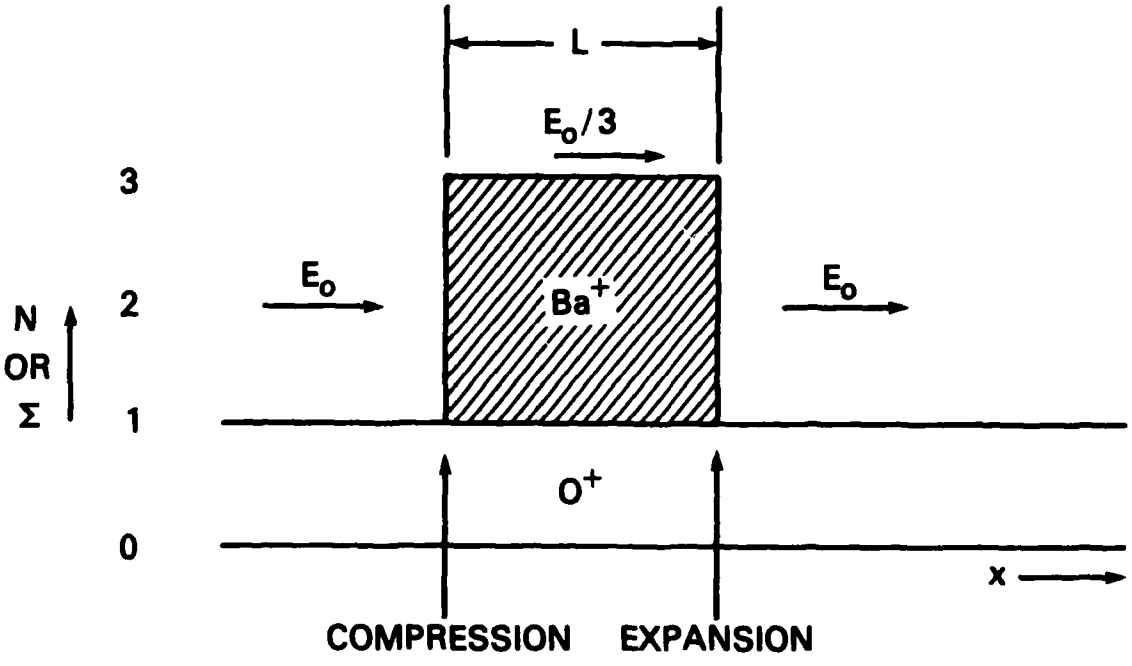

t_o = TIME FOR Ba^+ IONS TO LEAVE SLAB

$$= \frac{L}{\frac{\nu_{in}}{\Omega_i}\,\frac{c\,E_o}{3B}}$$

Fig. 2(a) — Schematic of a barium cloud in an ionosphere consisting of 0^+ ions, similar to Fig. 1 except that now we are in a "slab" geometry (plasma has infinite extent in y direction). The barium ions are shown cross-hatched while the oxygen ions are shown without cross-hatching. The shielding by the cloud causes a compression of ions to take place at the left edge and an expansion to take place at the right edge. The envelope $n_o + n_b$ depicts the electron density n_e, which cannot change in time.

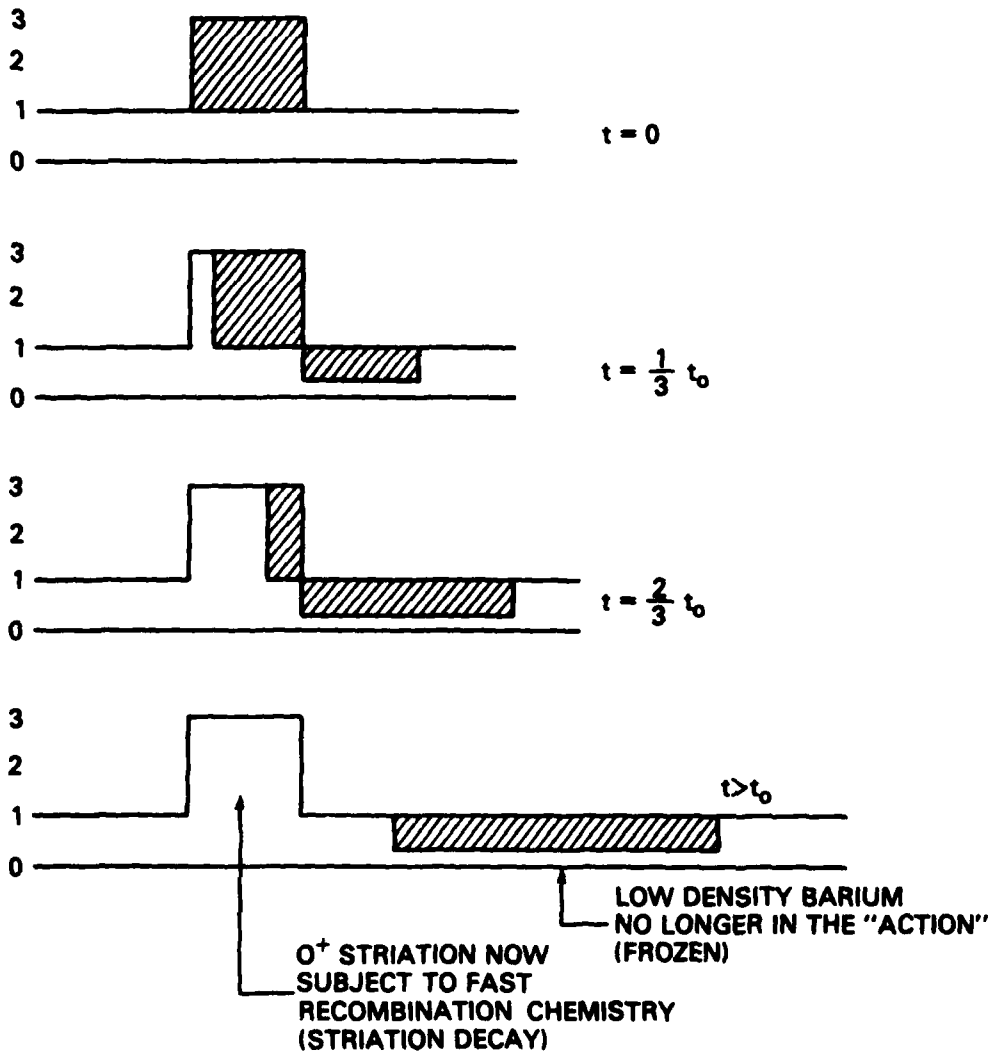

Fig. 2(b) — Time evolution of this cloud in units of t_o

to short chemical recombination times, this mechanism may very well result in the decay of the electron density cloud as well as the freezing of the barium cloud. This recombination effect is discussed in more detail in Prettie [1981].

We are now in a position to understand how it is that the barium that leaks from the electron cloud via the above mechanism appears in the form of sheets of barium leading the electron density cloud. Referring to Fig. 2a, we note that as the barium exits the right edge of the electron cloud, it experiences a factor of three increase in the rightward-directed electric field. It is the change in Pedersen drift associated with this which is responsible for the expansion of the ions as they exit the electron cloud. However it is precisely this same change in E which will produce a three-fold increase in the cE/B velocity of the ions toward the reader. Now consider the slice of barium located at $y = 0$ at $t = 0$. The right hand edge of this slice will immediately start moving toward the viewer at a velocity cE_o/B and to the right at velocity $(\nu_{bn}/\Omega_b)\ cE_o/B$. The left hand edge of this slice will move at precisely these same velocities but reduced by a factor of three. At time t_o when the barium has completely exited the electron cloud of width L, this slice will have its right hand and left hand coordinates located at $(x = 3L,\ y = -3\ \Omega_b \nu_{bn}^{-1}\ L)$ and $(x = 0,\ y = -\Omega_b \nu_{bn}^{-1}\ L)$ respectively, where we have defined $x = 0$ to be the right edge of the electron cloud. The barium slice is now 3L wide in the x direction and $2L\ \Omega_b \nu_{bn}^{-1}$ long in the y direction. For $\Omega_b \nu_{bn}^{-1} = 20$, we get a barium slice which is 13 times larger in y than it is in x. Referring to Fig. 1 we see that our postulated slice in Fig. 2 is analogous to the barium cloud itself in Fig. 1, so that again we expect the barium which has leaked out of the electron cloud to be much longer in the y direction than in the x direction, a geometry we could easily term a "sheet". The process is quite similar to what would happen if one were to eject a column of smoke sidewards from a moving automobile: the trail of smoke would be much larger along the direction of travel than tranverse to it. From the frame of reference of the electron cloud in Fig. 1, we are injecting a column of barium "smoke" transverse to our direction of travel relative to the ambient plasma. Hence the "trails" of barium.

Prettie [1981] has suggested that the barium sheets are the result of image formation and the resultant "quadrupole" electric fields. While we

would be the last to suggest that image formation is not important in barium cloud striations [Scannapieco et al., 1976; Ossakow et al., 1980], we believe the above shows the explanation to be quite a bit simpler. Numerical simulations to be presented in section 5 also bear this out.

4. The Pedersen Leakage Mechanism: More General Ionospheric Parameters

In the last section we confined ourselves to the case of two ion species, each of which had the same value of $\nu_{\alpha n}/\Omega_\alpha$. In this section we relax this last constraint for the purposes of a short qualitative discussion. A more detailed discussion of this topic, as well as a treatment of the case of more than two levels will be given in a future paper.

To illustrate the principles involved, we shall again use the one-dimensional slab depicted in Fig. 2, with the understanding that there is no longer a one-to-one correspondence between electron density n_e and total Pedersen conductivity $\Sigma_p \equiv \Sigma_{pb} + \Sigma_{po}$. Hence we shall interpret Fig. 2 to depict the n_e profile, with the Σ_p profile depending on the ion species involved, and which is, as we shall see, time dependent.

The principle to have in mind when analyzing the general case is that the electrons cannot move to the left or right, since they have no Pedersen mobility. Hence the electron density profile n_e is invariant in time as depicted in Fig. 2b. Since $n_b + n_o = n_e$, the B_a^+ and 0^+ ions are constrained to move in such a way as to maintain this invariance in n_e. In addition, the velocity of each ion species must be proportional to the electric field and to the appropriate $\nu_{\alpha n}/\Omega_\alpha$. Furthermore, the electric field must be inversely proportional to Σ_p.

The problem posed above for the general case $\nu_{bn}/\Omega_b \neq \nu_{on}/\Omega_o$ can be solved exactly. We shall not give the proof here, but simply state the remarkably simple result: The time evolution depicted in Fig. 2b for the special case $\nu_{bn}/\Omega_b = \nu_{on}/\Omega_o$ is in fact the general solution for $\nu_{bn}/\Omega_b \neq \nu_{on}/\Omega_o$, except for a change in temporal scaling. Specifically,

$$n_b' = f\, n_b^o \tag{4.1}$$

$$n_o' = f\, n_o^o \tag{4.2}$$

$$n_o'' = f^{-1} n_o^o = n_o^o + n_b^o \tag{4.3}$$

$$n_b'' = 0 \tag{4.4}$$

$$t_o = LB\Omega_b/(\nu_{bn} cE') \tag{4.5}$$

$$E' = E_o/M^o \tag{4.6}$$

$$f \equiv n_o^o/(n_o^o + n_b^o) \tag{4.7}$$

$$M^o \equiv (n_o^o \nu_{on} \Omega_o^{-1} + n_b^o \nu_{bn} \Omega_b^{-1})/(n_o^o \nu_{on} \Omega_o^{-1}) \tag{4.8}$$

where the prime superscript on n denotes quantities evaluated within the expanded barium cloud at time $t > t_o$ shown in Fig. 2b, the double prime superscript denotes quantities within the electron cloud at $t > t_o$ in the same figure, the zero superscript denotes quantities at time $t = 0$, and t_o is, as before, the time taken for the barium cloud to leave the electron cloud. Note that this says that the barium will <u>always</u> leave the electron cloud, but since t_o is proportional to $M^o/(\nu_{bn}/\Omega_b)$ the process may take an extremely long time if M^o is large or ν_{bn}/Ω_b is small. Just as important, it says that the Pedersen conductivity ratio M of the barium and electron clouds to the ambient ionosphere will change in the general case:

$$M' = f M^o \tag{4.9}$$

$$M'' = f^{-1} \tag{4.10}$$

where the superscripts have the same meaning as above. Since $0 < f < 1$, and in some cases may be close to zero, the barium cloud will always suffer a decrease in M value, and in fact it is possible to have $M' < 1$, in which case the barium cloud would actually represent a Pedersen conductivity depletion. As for the electron cloud, its M value may decrease or increase or stay the same, depending on f. Sufficiently small f will result in large increases in M for the electron cloud, and is the basis for the freezing mechanism for the electron cloud proposed by <u>Ossakow et al.</u> [1981], since a large M has been shown to be associated with a resistance to further structuring on the part of the electron cloud [<u>McDonald et al.</u>, 1981].

The above examples, and the parameter study suggested by (4.1) to (4.10) provide us with a vivid indication of the richness of the physics in the general case of $\nu_{bn}/\Omega_b \neq \nu_{on}/\Omega_o$. This richness is further compounded when we model the physics using more than two layers or species of ions. We are presently undertaking these parameter studies to determine these multilayer effects on the morphology of barium cloud striations. However, the point of this section is not to show how different and interesting this regime is, but rather to show that there are certain aspects of the physics, namely the leakage of barium from the electron cloud and its subsequent reduction in density and Pedersen conductivity by a factor f (Eq. (4.1) and (4.10)), that are independent of whether $\nu_{bn}/\Omega_b = \nu_{on}/\Omega_o$.

5. Numerical Simulations

In this section we return to the case considered in section 3, that of $\nu_{bn}/\Omega_b = \nu_{on}/\Omega_o$. There are several reasons for this : First, we have shown in the previous section that the basic Pedersen mobility leakage mechanism proposed here is active independent of this assumption. Second, this is the implicit assumption made in the "one-level approximation", and it will be interesting to see what effects are missed when one only follows electrons. Finally this is the case for which "image effects" are absent, and it becomes impossible to argue, as does Prettie [1981], that image-induced quadrupole fields affect the formation of barium sheets. As the numerical simulations will show, well-defined sheets of barium are produced without any evidence of quadrupole fields.

The simulation was performed on a stretched grid with 43 and 120 grid points in the x and y directions respectively. The central 31 by 100 portion of the mesh was uniformly gridded with $\Delta x = \Delta y = 0.258$ km. The four boundaries of the grid were placed well away from the cloud (utilizing the stretched mesh) to ensure no influence of the boundaries on the evolution of the cloud. Boundary conditions on all plasma species were that the normal derivative vanished. Boundary conditions on ϕ were Dirichlet ($\phi = 0$) on the left and right boundaries, and Neumann ($\partial\phi/\partial y = 0$) at the top and bottom boundaries. Two ion species were used, Ba^+ and O^+, with a value of $\nu_{an}/\Omega_a = 0.06$ assigned to each. The quantity n_o was initially assigned a normalized value of 1.0, and the initial barium cloud is given by

$$n_b = 4.0 \exp(- r^4/L^4)(1+P(x)) \tag{5.1}$$

$$r^2 = (x-x_o)^2 + (y-y_o)^2 \tag{5.2}$$

$$L = 2.5 \text{ km} \tag{5.3}$$

$$P(x) = 0.05 \cos(20(x-x_o)/L) \tag{5.4}$$

where the point (x_o,y_o) specifies the initial center of the cloud. The magnetic field $\underline{B}$ is taken to be 0.5 gauss directed along the positive $\hat{z}$ axis. The ambient electric field $\underline{E}_o$ is directed along the positive $\hat{x}$ axis with a magnitude such that $c\underline{E}_o \times \underline{B}/B^2$ is 100 m/sec directed along the negative $\hat{y}$ axis. The numerical resolution of this cloud is intentionally low, in order to allow us to run the calculation to late times at moderate cost. The inherent numerical dissipation of this low resolution has the effect of inhibiting bifurcation of the cloud but, as we shall see, this is actually an advantage since it allows us to see the leakage of the barium from the electron cloud in a "clean" calculation, without the complicating effects of cloud bifurcation.

Figure 3 shows isodensity contours of n_e (cross-hatched, denoted "Density 1") and n_b (denoted "Density 2") at various times during the calculation. The slight asymmetry in the electron density plots is due to the Hall terms in the potential equation. All calculations are performed in a reference frame moving with the electron cloud center of mass. Note that at time t = 0 sec the barium and electron contours are centered on one another, but that as time progresses the barium shows its inevitable drift to the right, "leaking" out of the electron cloud. At the latest time shown, 1096 sec, virtually all of the barium has left the electron cloud and formed a long, low density sheet of barium plasma to the right of and leading the electron cloud. One feature of the sheet that is quite striking is the much larger transverse gradients of n_b on the left side of the sheet than on the right side. There exists the possibility of optical or radar measurements of this barium cloud interpreting this steep gradient as "frozen structure".

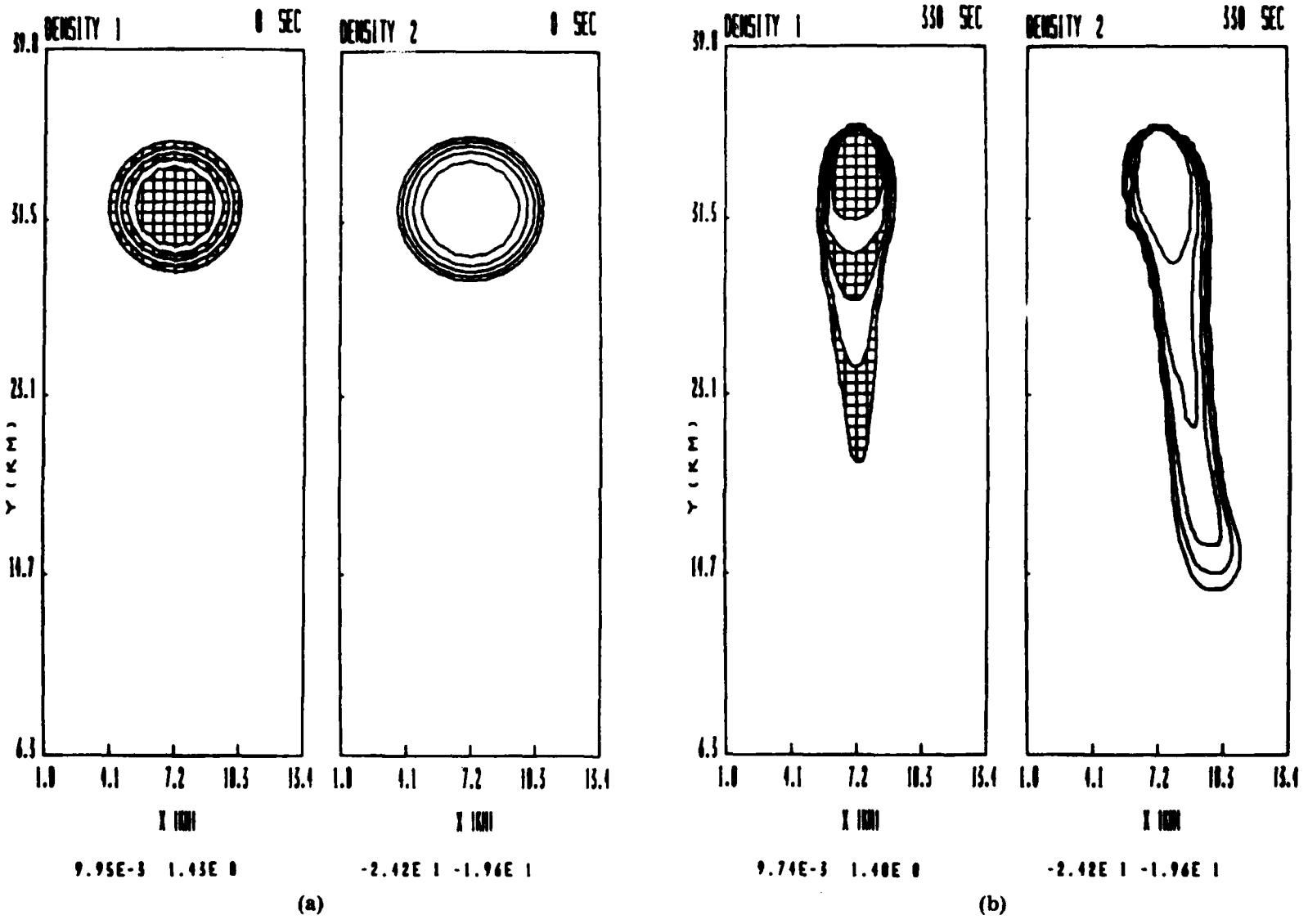

Fig. 3 — Evolution of the barium cloud described in the text computed via numerical simulation. Electron density contours (cross-hatched) are shown on the left, while contours of barium density are shown on the right. (a) 0 seconds (initial conditions) and (b) 330 seconds.

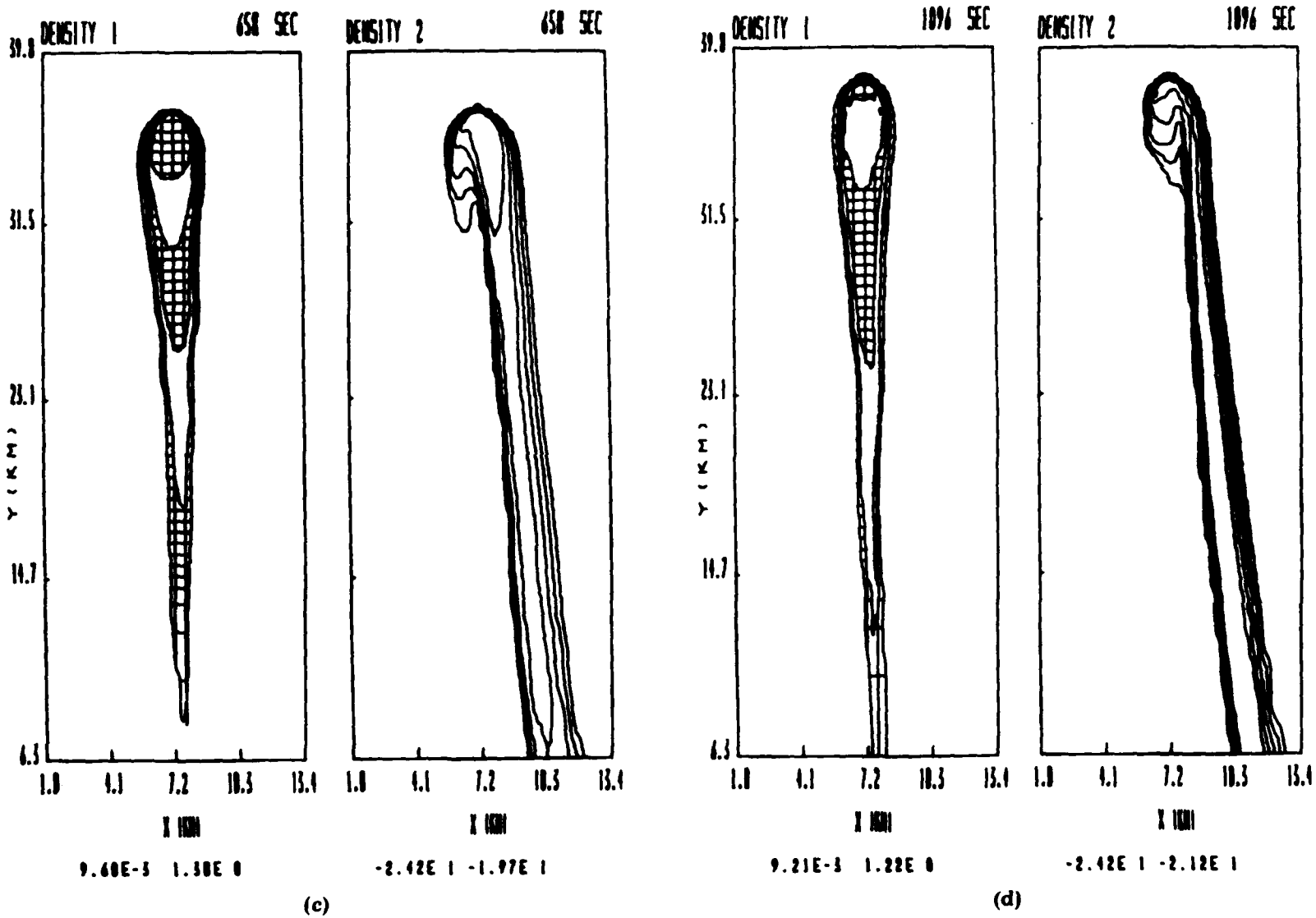

Fig. 3 (Cont'd) — Evolution of the barium cloud described in the text computed via numerical simulation. Electron density contours (cross-hatched) are shown on the left, while contours of barium density are shown on the right. (c) 658 seconds and (d) 1096 seconds.

A possible explanation of this feature is as follows. The barium comprising the right edge of the sheet originated near the right edge of the original barium cloud and thus was subject to some expansion as it left the electron cloud. Hence the right side of the sheet can be expected to have gradients as shallow or shallower than that of the original cloud. The barium comprising the left edge of the sheet originated on the left side of the original barium cloud and was therefore compressed in the x direction at first, resulting in a steepening of contours in the x direction. Subsequently the barium was expanded but this time in the y direction, a process which has no effect at all on the relative steepness of gradients in the x direction. Thus the steepness of the contours in the x direction is preserved. Fig. 4 we show contours of constant electrostatic potential ϕ at the same times as those used in Fig. 3. Notice the absence of any structure which might look even remotely like a "quadrupole".

It should be pointed out that while the density of the barium comprising the sheets may be somewhat low, it will appear bright optically to any observer whose line of sight is approximately parallel to the sheet orientation since the barium is optically thin and the integration path long. For a barium cloud driven by neutral winds, this will be the case for an observer anywhere near the initial cloud release site watching the cloud drift away at late times.

6. Conclusions and Future Work

We believe that we have shown the Pedersen drift mechanism proposed by Prettie [1981] and by Fedder (private communication, 1981) to be a viable candidate for barium cloud freezing. In addition we have shown that this mechanism can produce sheets of barium at late times which lead and are displaced from the electron cloud. We do not suggest, however, that this is the only possible mechanism. Indeed, we have proposed alternative mechanisms ourselves, and are presently considering still others. Nonetheless the mechanism looks sufficiently promising to merit further study. Certainly higher resolution numerical studies are in order, along with parameter studies of the effects of the relative Pedersen mobilities of the barium and ionospheric constituents. We hope to report on these in the near future.

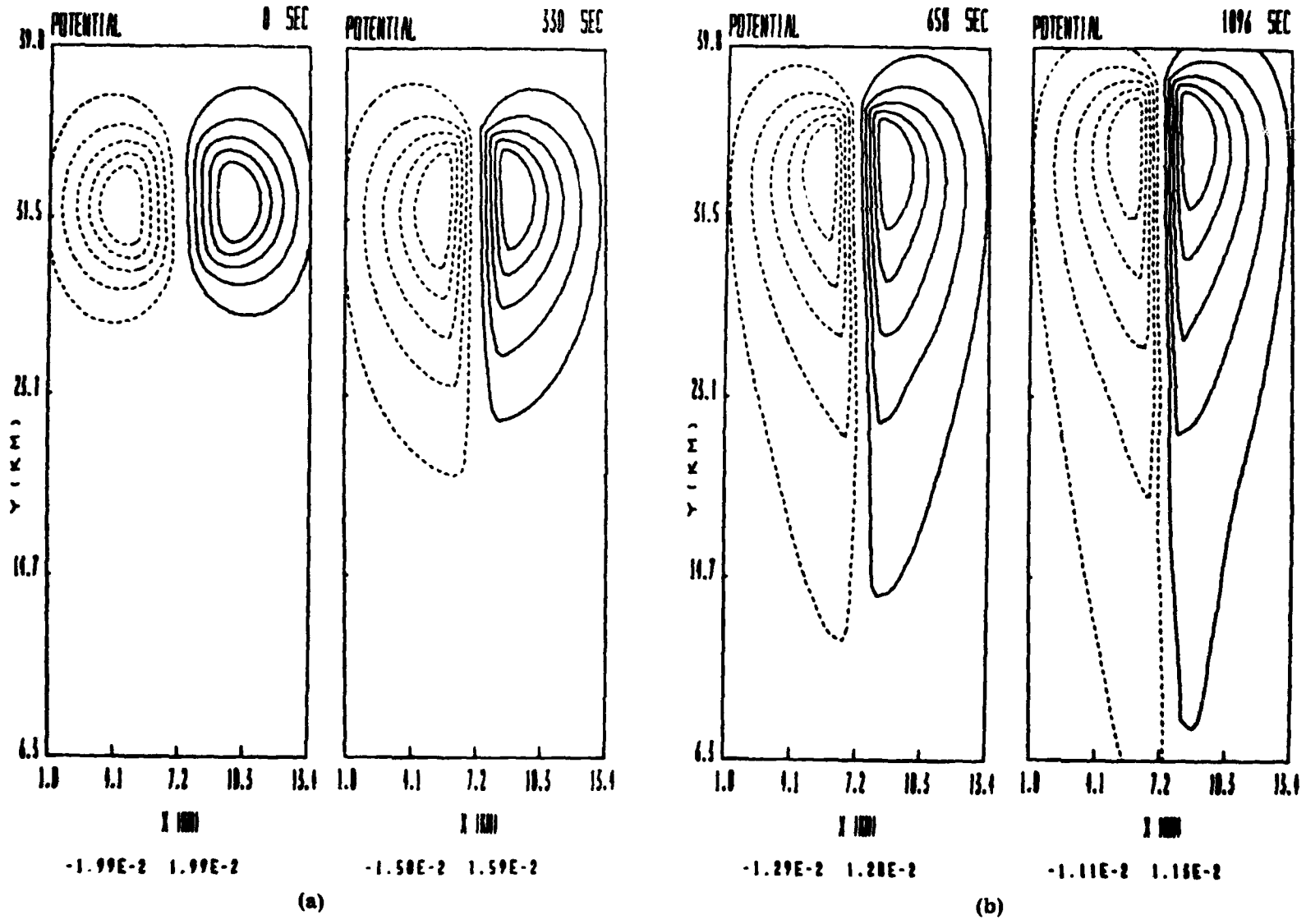

Fig. 4 — Contours of electrostatic potential ϕ for the calculation shown in Fig. 3. Positive values of ϕ are contoured with solid lines, while negative values are contoured as dashed lines. Note the absence of any quadrupolar components. (a) Contours at 0 and 330 seconds and (b) contours at 658 and 1096 seconds.

Acknowledgment

This work was sponsored by the Defense Nuclear Agency.

References

Goldman, S.R., S.L. Ossakow, and D.L. Book, On the nonlinear motion of a small barium cloud in the ionosphere, J. Geophys. Res., 79, 1471, 1974.

Lloyd, K.H., and G. Haerendel, Numerical modeling of the drift and deformation of ionospheric plasma clouds and of their interaction with other layers of the ionosphere, J. Geophys. Res., 78, 7389, 1973.

McDonald, B.E., M.J. Keskinen, S.L. Ossakow, and S.T. Zalesak, Computer simulation of gradient drift processes in operation Avefria, J. Geophys. Res., 85, 2143, 1980.

McDonald, B.E., S.L. Ossakow, S.T. Zalesak, and N.J. Zabusky, Scale sizes and lifetimes of F region plasma cloud striations as determined by the condition of marginal stability, J. Geophys. Res., 86, 5775, 1981.

Ossakow, S.L., Ionospheric irregularities, Rev. Geophys. Space Phys., 17, 521, 1979.

Ossakow, S.L., S.T. Zalesak, and M.J. Keskinen, A plausible hypothesis for striation freezing in ionospheric plasma clouds, Memo Report 4597, Nav. Res. Lab., Washington, D.C., Aug., 1981.

Ossakow, S.L., M.J. Keskinen, and S.T. Zalesak, Ionspheric irregularity physics modelling, AIAA-82-0147, January, 1982.

Perkins, F.W., N.J. Zabusky, and J.H. Doles III, Deformation and striation of plasma clouds in the ionosphere, 1, J. Geophys. Res., 78, 697, 1973.

Prettie, C., A. Johnson, J. Marshall, T. Grizinski, and R. Swanson, Project STRESS satellite communication test results, Tech. Rep., 77-158, Air Force Avionics Lab., Wright-Patterson Air Force Base, Ohio, July, 1977.

Prettie, C.W., New understanding in the evolution of ionospheric plasma clouds, Berkeley Research Associates preprint, Nov., 1981.

Scannapieco, A.J., S.L. Ossakow, S.R. Goldman, and J.M. Pierre, Plasma cloud late-time striation spectra, J. Geophys. Res., 81, 6037, 1976.

DISTRIBUTION LIST

DEPARTMENT OF DEFENSE

ASSISTANT SECRETARY OF DEFENSE
COMM, CMD, CONT 7 INTELL
WASHINGTON, D.C. 20301
01CY ATTN J. BABCOCK
01CY ATN M. EPSTEIN

DIRECTOR
COMMAND CONTROL TECHNICAL CENTER
PENTAGON RM BE 685
WASHINGTON, D.C. 20301
01CY ATTN C-650
01CY ATTN C-312 R. MASON

DIRECTOR
DEFENSE ADVANCED RSCH PROJ AGENCY
ARCHITECT BUILDING
1400 WILSON BLVD.
ARLINGTON, VA. 22209
01CY ATTN NUCLEAR MONITORING RESEARCH
01CY ATTN STRATEGIC TECH OFFICE

DEFENSE COMMUNICATION ENGINEER CENTER
1860 WIEHLE AVENUE
RESTON, VA. 22090
01CY ATTN CODE R410
01CY ATTN CODE R812

DIRECTOR
DEFENSE COMMUNICATIONS AGENCY
WASHINGTON, D.C. 20305
(ADR CNWDI: ATTN CODE 240 FOR)
01CY ATTN CODE 101B

DEFENSE TECHNICAL INFORMATION CENTER
CAMERON STATION
ALEXANDRIA, VA. 22314
02CY

DIRECTOR
DEFENSE NUCLEAR AGENCY
WASHINGTON, D.C. 20305
01CY ATTN STVL
04CY ATTN TITL
01CY ATTN DDST
03CY ATTN RAAE

COMMANDER
FIELD COMMAND
DEFENSE NUCLEAR AGENCY
KIRTLAND, AFB, NM 87115
01CY ATTN FCPR

DIRECTOR
INTERSERVICE NUCLEAR WEAPONS SCHOOL
KIRTLAND AFB, NM 87115
01CY ATTN DOCUMENT CONTROL

JOINT CHIEFS OF STAFF
WASHINGTON, D.C. 20301
01CY ATTN J-3 WWMCCS EVALUATION OFFICE

DIRECTOR
JOINT STRAT TGT PLANNING STAFF
OFFUTT AFB
OMAHA, NB 68113
01CY ATTN JLTW-2
01CY ATTN JPST G. GOETZ

CHIEF
LIVERMORE DIVISION FLD COMMAND DNA
DEPARTMENT OF DEFENSE
LAWRENCE LIVERMORE LABORATORY
P.O. BOX 808
LIVERMORE, CA 94550
01CY ATTN FCPRL

COMMANDANT
NATO SCHOOL (SHAPE)
APO NEW YORK 09172
01CY ATTN U.S. DOCUMENTS OFFICER

UNDER SECY OF DEF FOR RSCH & ENGRG
DEPARTMENT OF DEFENSE
WASHINGTON, D.C. 20301
01CY ATTN STRATEGIC & SPACE SYSTEMS (OS)

WWMCCS SYSTEM ENGINEERING ORG
WASHINGTON, D.C. 20305
01CY ATTN R. CRAWFORD

COMMANDER/DIRECTOR
ATMOSPHERIC SCIENCES LABORATORY
U.S. ARMY ELECTRONICS COMMAND
WHITE SANDS MISSILE RANGE, NM 88002
01CY ATTN DELAS-EO F. NILES

DIRECTOR
BMD ADVANCED TECH CTR
HUNTSVILLE OFFICE
P.O. BOX 1500
HUNTSVILLE, AL 35807
01CY ATTN ATC-T MELVIN T. CAPPS
01CY ATTN ATC-O W. DAVIES
01CY ATTN ATC-R DON RUSS

PROGRAM MANAGER
BMD PROGRAM OFFICE
5001 EISENHOWER AVENUE
ALEXANDRIA, VA 22333
01CY ATTN DACS-BMT J. SHEA

CHIEF C-E- SERVICES DIVISION
U.S. ARMY COMMUNICATIONS CMD
PENTAGON RM 1B269
WASHINGTON, D.C. 20310
01CY ATTN C- E-SERVICES DIVISION

COMMANDER
FRADCOM TECHNICAL SUPPORT ACTIVITY
DEPARTMENT OF THE ARMY
FORT MONMOUTH, N.J. 07703
01CY ATTN DRSEL-NL-RD H. BENNET
01CY ATTN DRSEL-PL-ENV H. BOMKE
01CY ATTN J.E. QUIGLEY

COMMANDER
HARRY DIAMOND LABORATORIES
DEPARTMENT OF THE ARMY
2800 POWDER MILL ROAD
ADELPHI, MD 20783
(CNWDI-INNER ENVELOPE: ATTN: DELHD-RBH)
01CY ATTN DELHD-TI M. WEINER
01CY ATTN DELHD-RB R. WILLIAMS
01CY ATTN DELHD-NP F. WIMENITZ
01CY ATTN DELHD-NP C. MOAZED

COMMANDER
U.S. ARMY COMM-ELEC ENGRG INSTAL AGY
FT. HUACHUCA, AZ 85613
01CY ATTN CCC-EMEO GEORGE LANE

COMMANDER
U.S. ARMY FOREIGN SCIENCE & TECH CTR
220 7TH STREET, NE
CHARLOTTESVILLE, VA 22901
01CY ATTN DRXST-SD
01CY ATTN R. JONES

COMMANDER
U.S. ARMY MATERIAL DEV & READINESS CMD
5001 EISENHOWER AVENUE
ALEXANDRIA, VA 22333
01CY ATTN DRCLDC J.A. BENDER

COMMANDER
U.S. ARMY NUCLEAR AND CHEMICAL AGENCY
7500 BACKLICK ROAD
BLDG 2073
SPRINGFIELD, VA 22150
01CY ATTN LIBRARY

DIRECTOR
U.S. ARMY BALLISTIC RESEARCH LABORATORY
ABERDEEN PROVING GROUND, MD 21005
01CY ATTN TECH LIBRARY EDWARD BAICY

COMMANDER
U.S. ARMY SATCOM AGENCY
FT. MONMOUTH, NJ 07703
01CY ATTN DOCUMENT CONTROL

COMMANDER
U.S. ARMY MISSILE INTELLIGENCE AGENCY
REDSTONE ARSENAL, AL 35809
01CY ATTN JIM GAMBLE

DIRECTOR
U.S. ARMY TRADOC SYSTEMS ANALYSIS ACTIVITY
WHITE SANDS MISSILE RANGE, NM 88002
01CY ATTN ATAA-SA
01CY ATTN TCC/F. PAYAN JR.
01CY ATTN ATTA-TAC LTC J. HESSE

COMMANDER
NAVAL ELECTRONIC SYSTEMS COMMAND
WASHINGTON, D.C. 20360
01CY ATTN NAVALEX 034 T. HUGHES
01CY ATTN PME 117
01CY ATTN PME 117-T
01CY ATTN CODE 5011

COMMANDING OFFICER
NAVAL INTELLIGENCE SUPPORT CTR
4301 SUITLAND ROAD, BLDG. 5
WASHINGTON, D.C. 20390
01CY ATTN MR. DUBBIN STIC 12
01CY ATTN NISC-50
01CY ATTN CODE 5404 J. GALET

COMMANDER
NAVAL OCCEAN SYSTEMS CENTER
SAN DIEGO, CA 92152
03CY ATTN CODE 532 W. MOLER
01CY ATTN CODE 0230 C. BAGGETT
01CY ATTN CODE 81 R. EASTMAN

DIRECTOR
NAVAL RESEARCH LABORATORY
WASHINGTON, D.C. 20375
01CY ATTN CODE 4700 S. L. Ossakow
26 CYS IF UNCLASS. 1 CY IF CLASS)
01CY ATTN CODE 4701 JACK D. BROWN
01CY ATTN CODE 4780 BRANCH HEAD (150
CYS IF UNCLASS, 1 CY IF CLASS)
01CY ATTN CODE 7500
01CY ATTN CODE 7550
01CY ATTN CODE 7580
01CY ATTN CODE 7551
01CY ATTN CODE 7555
01CY ATTN CODE 4730 E. MCLEAN
01CY ATTN CODE 4187

COMMANDER
NAVAL SEA SYSTEMS COMMAND
WASHINGTON, D.C. 20362
01CY ATTN CAPT R. PITKIN

COMMANDER
NAVAL SPACE SURVEILLANCE SYSTEM
DAHLGREN, VA 22448
01CY ATTN CAPT J.H. BURTON

OFFICER-IN-CHARGE
NAVAL SURFACE WEAPONS CENTER
WHITE OAK, SILVER SPRING, MD 20910
01CY ATTN CODE F31

DIRECTOR
STRATEGIC SYSTEMS PROJECT OFFICE
DEPARTMENT OF THE NAVY
WASHINGTON, D.C. 20376
01CY ATTN NSP-2141
01CY ATTN NSSP-2722 FRED WIMBERLY

COMMANDER
NAVAL SURFACE WEAPONS CENTER
DAHLGREN LABORATORY
DAHLGREN, VA 22448
01CY ATTN CODE DF-14 R. BUTLER

OFFICER OF NAVAL RESEARCH
ARLINGTON, VA 22217
01CY ATTN CODE 465
01CY ATTN CODE 461
01CY ATTN CODE 402
01CY ATTN CODE 420
01CY ATTN CODE 421

COMMANDER
AEROSPACE DEFENSE COMMAND/DC
DEPARTMENT OF THE AIR FORCE
ENT AFB, CO 80912
01CY ATTN DC MR. LONG

COMMANDER
AEROSPACE DEFENSE COMMAND/XPD
DEPARTMENT OF THE AIR FORCE
ENT AFB, CO 80912
01CY ATTN XPDQQ
01CY ATTN XP

AIR FORCE GEOPHYSICS LABORATORY
HANSCOM AFB, MA 01731
01CY ATTN OPR HAROLD GARDNER
01CY ATTN LKB KENNETH S.W. CHAMPION
01CY ATTN OPR ALVA T. STAIR
01CY ATTN PHP JULES AARONS
01CY ATTN PHD JURGEN BUCHAU
01CY ATTN PHD JOHN P. MULLEN

AF WEAPONS LABORATORY
KIRTLAND AFT, NM 87117
01CY ATTN SUL
01CY ATTN CA ARTHUR H. GUENTHER
01CY ATTN NTYCE 1LT. G. KRAJEI

AFTAC
PATRICK AFB, FL 32925
01CY ATTN TF/MAJ WILEY
01CY ATTN TN

AIR FORCE AVIONICS LABORATORY
WRIGHT-PATTERSON AFB, OH 45433
01CY ATTN AAD WADE HUNT
01CY ATTN AAD ALLEN JOHNSON

DEPUTY CHIEF OF STAFF
RESEARCH, DEVELOPMENT, & ACQ
DEPARTMENT OF THE AIR FORCE
WASHINGTON, D.C. 20330
01CY ATTN AFRDQ

HEADQUATERS
ELECTRONIC SYSTEMS DIVISION/XR
DEPARTMENT OF THE AIR FORCE
HANSCOM AFB, MA 01731
01CY ATTN XR J. DEAS

HEADQUATERS
ELECTRONIC SYSTEMS DIVISION/YSEA
DEPARTMENT OF THE AIR FORCE
HANSCOM AFB, MA 01732
01CY ATTN YSEA

HEADQUATERS
ELECTRONIC SYSTEMS DIVISION/DC
DEPARTMENT OF THE AIR FORCE
HANSCOM AFB, MA 01731
01CY ATTN DCKC MAJ J.C. CLARK

COMMANDER
FOREIGN TECHNOLOGY DIVISION, AFSC
WRIGHT-PATTERSON AFB, OH 45433
01CY ATTN NICD LIBRARY
01CY ATTN ETDP B. BALLARD

COMMANDER
ROME AIR DEVELOPMENT CENTER, AFSC
GRIFFISS AFB, NY 13441
01CY ATTN DOC LIBRARY/TSLD
01CY ATTN OCSE V. COYNE

SAMSO/SZ
POST OFFICE BOX 92960
WORLDWAY POSTAL CENTER
LOS ANGELES, CA 90009
(SPACE DEFENSE SYSTEMS)
01CY ATTN SZJ

STRATEGIC AIR COMMAND/XPFS
OFFUTT AFB, NB 68113
01CY ATTN XPFS MAJ B. STEPHAN
01CY ATTN ADWATE MAJ BRUCE BAUER
01CY ATTN NRT
01CY ATTN DOK CHIEF SCIENTIST

SAMSO/SK
P.O. BOX 92960
WORLDWAY POSTAL CENTER
LOS ANGELES, CA 90009
01CY ATTN SKA (SPACE COMM SYSTEMS)
M. CLAVIN

SAMSO/MN
NORTON AFB, CA 92409
(MINUTEMAN)
01CY ATTN MNNL LTC KENNEDY

COMMANDER
ROME AIR DEVELOPMENT CENTER, AFSC
HANSCOM AFB, MA 01731
01CY ATTN EEP A. LORENTZEN

DEPARTMENT OF ENERGY
LIBRARY ROOM G-042
WASHINGTON, D.C. 20545
01CY ATTN DOC CON FOR A. LABOWITZ

DEPARTMENT OF ENERGY
ALBUQUERQUE OPERATIONS OFFICE
P.O. BOX 5400
ALBUQUERQUE, NM 87115
01CY ATTN DOC CON FOR D. SHERWOOD

EG&G, INC.
LOS ALAMOS DIVISION
P.O. BOX 809
LOS ALAMOS, NM 85544
01CY ATTN DOC CON FOR J. BREEDLOVE

UNIVERSITY OF CALIFORNIA
LAWRENCE LIVERMORE LABORATORY
P.O. BOX 808
LIVERMORE, CA 94550
01CY ATTN DOC CON FOR TECH INFO DEPT
01CY ATTN DOC CON FOR L-389 R. OTT
01CY ATTN DOC CON FOR L-31 R. HAGER
01CY ATTN DOC CON FOR L-46 F. SEWARD

LOS ALAMOS NATIONAL LABORATORY
P.O. BOX 1663
LOS ALAMOS, NM 87545
01CY ATTN DOC CON FOR J. WOLCOTT
01CY ATTN DOC CON FOR R.F. TASCHEK
01CY ATTN DOC CON FOR E. JONES
01CY ATTN DOC CON FOR J. MALIK
01CY ATTN DOC CON FOR R. JEFFRIES
01CY ATTN DOC CON FOR J. ZINN
01CY ATTN DOC CON FOR P. KEATON
01CY ATTN DOC CON FOR D. WESTERVELT

SANDIA LABORATORIES
P.O. BOX 5800
ALBUQUERQUE, NM 87115
01CY ATTN DOC CON FOR W. BROWN
01CY ATTN DOC CON FOR A. THORNBROUGH
01CY ATTN DOC CON FOR T. WRIGHT
01CY ATTN DOC CON FOR D. DAHLGREN
01CY ATTN DOC CON FOR 3141
01CY ATTN DOC CON FOR SPACE PROJECT DIV

SANDIA LABORATORIES
LIVERMORE LABORATORY
P.O. BOX 969
LIVERMORE, CA 94550
01CY ATTN DOC CON FOR B. MURPHEY
01CY ATTN DOC CON FOR T. COOK

OFFICE OF MILITARY APPLICATION
DEPARTMENT OF ENERGY
WASHINGTON, D.C. 20545
01CY ATTN DOC CON DR. YO SONG

OTHER GOVERNMENT

DEPARTMENT OF COMMERCE
NATIONAL BUREAU OF STANDARDS
WASHINGTON, D.C. 20234
(ALL CORRES: ATTN SEC OFFICER FOR)
01CY ATTN R. MOORE

INSTITUTE FOR TELECOM SCIENCES
NATIONAL TELECOMMUNICATIONS & INFO ADMIN
BOULDER, CO 80303
01CY ATTN A. JEAN (UNCLASS ONLY)
01CY ATTN W. UTLAUT
01CY ATTN D. CROMBIE
01CY ATTN L. BERRY

NATIONAL OCEANIC & ATMOSPHERIC ADMIN
ENVIRONMENTAL RESEARCH LABORATORIES
DEPARTMENT OF COMMERCE
BOULDER, CO 80302
01CY ATTN R. GRUBB
01CY ATTN AERONOMY LAB G. REID

DEPARTMENT OF DEFENSE CONTRACTORS

AEROSPACE CORPORATION
P.O. BOX 92957
LOS ANGELES, CA 90009
01CY ATTN I. GARFUNKEL
01CY ATTN T. SALMI
01CY ATTN V. JOSEPHSON
01CY ATTN S. BOWER
01CY ATTN N. STOCKWELL
01CY ATTN D. OLSEN

ANALYTICAL SYSTEMS ENGINEERING CORP
5 OLD CONCORD ROAD
BURLINGTON, MA 01803
01CY ATTN RADIO SCIENCES

BERKELEY RESEARCH ASSOCIATES, INC.
P.O. BOX 983
BERKELEY, CA 94701
01CY ATTN J. WORKMAN
01CY ATTN C. PRETTIE

BOEING COMPANY, THE
P.O. BOX 3707
SEATTLE, WA 98124
01CY ATTN G. KEISTER
01CY ATTN D. MURRAY
01CY ATTN G. HALL
01CY ATTN J. KENNEY

BROWN ENGINEERING COMPANY, INC.
CUMMINGS RESEARCH PARK
HUNTSVILLE, AL 35807
01CY ATTN ROMEO A. DELIBERIS

CALIFORNIA AT SAN DIEGO, UNIV OF
P.O. BOX 6049
SAN DIEGO, CA 92106

CHARLES STARK DRAPER LABORATORY, INC.
555 TECHNOLOGY SQUARE
CAMBRIDGE, MA 02139
01CY ATTN D.B. COX
01CY ATTN J.P. GILMORE

COMSAT LABORATORIES
LINTHICUM ROAD
CLARKSBURG, MD 20734
01CY ATTN G. HYDE

CORNELL UNIVERSITY
DEPARTMENT OF ELECTRICAL ENGINEERING
ITHACA, NY 14850
01CY ATTN D.T. FARLEY, JR.

ELECTROSPACE SYSTEMS, INC.
BOX 1359
RICHARDSON, TX 75080
01CY ATTN H. LOGSTON
01CY ATTN SECURITY (PAUL PHILLIPS)

ESL, INC.
495 JAVA DRIVE
SUNNYVALE, CA 94086
01CY ATTN J. ROBERTS
01CY ATTN JAMES MARSHALL

GENERAL ELECTRIC COMPANY
SPACE DIVISION
VALLEY FORGE SPACE CENTER
GODDARD BLVD KING OF PRUSSIA
P.O. BOX 8555
PHILADELPHIA, PA 19101
01CY ATTN M.H. BORTNER SPACE SCI LAB

GENERAL ELECTRIC COMPANY
P.O. BOX 1122
SYRACUSE, NY 13201
01CY ATTN F. REIBERT

GENERAL ELECTRIC TECH SERVICES CO., INC.
HMES
COURT STREET
SYRACUSE, NY 13201
01CY ATTN G. MILLMAN

GENERAL RESEARCH CORPORATION
SANTA BARBARA DIVISION
P.O. BOX 6770
SANTA BARBARA, CA 93111
01CY ATTN JOHN ISE, JR.
01CY ATTN JOEL GARBARINO

GEOPHYSICAL INSTITUTE
UNIVERSITY OF ALASKA
FAIRBANKS, AK 99701
(ALL CLASS ATTN: SECURITY OFFICER)
01CY ATTN T.N. DAVIS (UNCLASS ONLY)
01CY ATTN TECHNICAL LIBRARY
01CY ATTN NEAL BROWN (UNCLASS ONLY)

GTE SYLVANIA, INC.
ELECTRONICS SYSTEMS GRP-EASTERN DIV
77 A STREET
NEEDHAM, MA 02194
01CY ATTN MARSHALL CROSS

HSS, INC.
2 ALFRED CIRCLE
BEDFORD, MA 01730
01CY ATTN DONALD HANSEN

ILLINOIS, UNIVERSITY OF
107 COBLE HALL
150 DAVENPORT HOUSE
CHAMPAIGN, IL 61820
(ALL CORRES ATTN DAN MCCLELLAND)
01CY ATTN K. YEH

INSTITUTE FOR DEFENSE ANALYSES
400 ARMY-NAVY DRIVE
ARLINGTON, VA 22202
01CY ATTN J.M. AEIN
01CY ATTN ERNEST BAUER
01CY ATTN HANS WOLFARD
01CY ATTN JOEL BENGSTON

INTL TEL & TELEGRAPH CORPORATION
500 WASHINGTON AVENUE
NUTLEY, NJ 07110
01CY ATTN TECHNICAL LIBRARY

JAYCOR
11011 TORREYANA ROAD
P.O. BOX 85154
SAN DIEGO, CA 92138
01CY ATTN J.L. SPERLING

JOHNS HOPKINS UNIVERSITY
APPLIED PHYSICS LABORATORY
JOHNS HOPKINS ROAD
LAUREL, MD 20707
01CY ATTN DOCUMENT LIBRARIAN
01CY ATTN THOMAS POTEMRA
01CY ATTN JOHN DASSOULAS
01CY ATTN DR. DONALD J. WILLIAMS

KAMAN SCIENCES CORP
P.O. BOX 7463
COLORADO SPRINGS, CO 80933
01CY ATTN T. MEAGHER

KAMAN TEMPO-CENTER FOR ADVANCED STUDIES
816 STATE STREET (P.O DRAWER QQ)
SANTA BARBARA, CA 93102
01CY ATTN DASIAC
01CY ATTN TIM STEPHANS
01CY ATTN WARREN S. KNAPP
01CY ATTN WILLIAM MCNAMARA
01CY ATTN B. GAMBILL

LINKABIT CORP
10453 ROSELLE
SAN DIEGO, CA 92121
01CY ATTN IRWIN JACOBS

LOCKHEED MISSILES & SPACE CO., INC
P.O. BOX 504
SUNNYVALE, CA 94088
01CY ATTN DEPT 60-12
01CY ATTN D.R. CHURCHILL

LOCKHEED MISSILES & SPACE CO., INC.
3251 HANOVER STREET
PALO ALTO, CA 94304
01CY ATTN MARTIN WALT DEPT 52-12
01CY ATTN W.L. IMHOF DEPT 52-12
01CY ATTN RICHARD G. JOHNSON DEPT 52-12
01CY ATTN J.B. CLADIS DEPT 52-12

LOCKHEED MISSILE & SPACE CO., INC.
HUNTSVILLE RESEARCH & ENGR. CTR.
4800 BRADFORD DRIVE
HUNTSVILLE, AL 35807
ATTN DALE H. DIVIS

MARTIN MARIETTA CORP
ORLANDO DIVISION
P.O. BOX 5837
ORLANDO, FL 32805
01CY ATTN R. HEFFNER

M.I.T. LINCOLN LABORATORY
P.O. BOX 73
LEXINGTON, MA 02173
01CY ATTN DAVID M. TOWLE
01CY ATTN P. WALDRON
01CY ATTN L. LOUGHLIN
01CY ATTN D. CLARK

MCDONNEL DOUGLAS CORPORATION
5301 BOLSA AVENUE
HUNTINGTON BEACH, CA 92647
01CY ATTN N. HARRIS
01CY ATTN J. MOULE
01CY ATTN GEORGE MROZ
01CY ATTN W. OLSON
01CY ATTN R.W. HALPRIN
01CY ATTN TECHNICAL LIBRARY SERVICES

MISSION RESEARCH CORPORATION
735 STATE STREET
SANTA BARBARA, CA 93101
01CY ATTN P. FISCHER
01CY ATTN W.F. CREVIER
01CY ATTN STEVEN L. GUTSCHE
01CY ATTN D. SAPPENFIELD
01CY ATTN R. BOGUSCH
01CY ATTN R. HENDRICK
01CY ATTN RALPH KILB
01CY ATTN DAVE SOWLE
01CY ATTN F. FAJEN
01CY ATTN M. SCHEIBE
01CY ATTN CONRAD L. LONGMIRE
01CY ATTN WARREN A. SCHLUETER

MITRE CORPORATION, THE
P.O. BOX 208
BEDFORD, MA 01730
01CY ATTN JOHN MORGANSTERN
01CY ATTN G. HARDING
01CY ATTN C.E. CALLAHAN

MITRE CORP
WESTGATE RESEARCH PARK
1820 DOLLY MADISON BLVD
MCLEAN, VA 22101
01CY ATTN W. HALL
01CY ATTN W. FOSTER

PACIFIC-SIERRA RESEARCH CORP
1456 CLOVERFIELD BLVD.
SANTA MONICA, CA 90404
01CY ATTN E.C. FIELD, JR.

PENNSYLVANIA STATE UNIVERSITY
IONOSPHERE RESEARCH LAB
318 ELECTRICAL ENGINEERING EAST
UNIVERSITY PARK, PA 16802
(NO CLASS TO THIS ADDRESS)
01CY ATTN IONOSPHERIC RESEARCH LAB

PHOTOMETRICS, INC.
442 MARRETT ROAD
LEXINGTON, MA 02173
01CY ATTN IRVING L. KOFSKY

PHYSICAL DYNAMICS, INC.
P.O. BOX 3027
BELLEVUE, WA 98009
01CY ATTN E.J. FREMOUW

PHYSICAL DYNAMICS, INC.
P.O. BOX 10367
OAKLAND, CA 94610
ATTN A. THOMSON

R & D ASSOCIATES
P.O. BOX 9695
MARINA DEL REY, CA 90291
01CY ATTN FORREST GILMORE
01CY ATTN BRYAN GABBARD
01CY ATTN WILLIAM B. WRIGHT, JR.
01CY ATTN ROBERT F. LELEVIER
01CY ATTN WILLIAM J. KARZAS
01CY ATTN H. ORY
01CY ATTN C. MACDONALD
01CY ATTN R. TURCO

RAND CORPORATION, THE
1700 MAIN STREET
SANTA MONICA, CA 90406
01CY ATTN CULLEN CRAIN
01CY ATTN ED BEDROZIAN

RAYTHEON CO.
528 BOSTON POST ROAD
SUDBURY, MA 01776
01CY ATTN BARBARA ADAMS

RIVERSIDE RESEARCH INSTITUTE
80 WEST END AVENUE
NEW YORK, NY 10023
01CY ATTN VINCE TRAPANI

SCIENCE APPLICATIONS, INC.
P.O. BOX 2351
LA JOLLA, CA 92038
01CY ATTN LEWIS M. LINSON
01CY ATTN DANIEL A. HAMLIN
01CY ATTN E. FRIEMAN
01CY ATTN E.A. STRAKER
01CY ATTN CURTIS A. SMITH
01CY ATTN JACK MCDOUGALL

SCIENCE APPLICATIONS, INC
1710 GOODRIDGE DR.
MCLEAN, VA 22102
ATTN: J. COCKAYNE

SRI INTERNATIONAL
333 RAVENSWOOD AVENUE
MENLO PARK, CA 94025
01CY ATTN DONALD NEILSON
01CY ATTN ALAN BURNS
01CY ATTN G. SMITH
01CY ATTN L.L. COBB
01CY ATTN DAVID A. JOHNSON
01CY ATTN WALTER G. CHESNUT
01CY ATTN CHARLES L. RINO
01CY ATTN WALTER JAYE
01CY ATTN M. BARON
01CY ATTN RAY L. LEADABRAND
01CY ATTN G. CARPENTER
01CY ATTN G. PRICE
01CY ATTN J. PETERSON
01CY ATTN R. HAKE, JR.
01CY ATTN V. GONZALES
01CY ATTN D. MCDANIEL

STEWART RADIANCE LABORATORY
UTAH STATE UNIVERSITY
1 DE ANGELO DRIVE
BEDFORD, MA 01730
01CY ATTN J. ULWICK

TECHNOLOGY INTERNATIONAL CORP
75 WIGGINS AVENUE
BEDFORD, MA 01730
01CY ATTN W.P. BOQUIST

TRW DEFENSE & SPACE SYS GROUP
ONE SPACE PARK
REDONDO BEACH, CA 90278
01CY ATTN R. K. PLEBUCH
01CY ATTN S. ALTSCHULER
01CY ATTN D. DEE

VISIDYNE
SOUTH BEDFORD STREET
BURLINGTON, MASS 01803
01CY ATTN W. REIDY
01CY ATTN J. CARPENTER
01CY ATTN C. HUMPHREY

IONOSPHERIC MODELING DISTRIBUTION LIST
(UNCLASSIFIED ONLY)

PLEASE DISTRIBUTE ONE COPY TO EACH OF THE FOLLOWING PEOPLE:

NAVAL RESEARCH LABORATORY
WASHINGTON, D.C. 20375
- DR. P. MANGE - CODE 4101
- DR. R. MEIER - CODE 4141
- DR. E. SZUSZCZEWICZ - CODE 4187
- DR. J. GOODMAN - CODE 4180
- DR. R. RODRIGUEZ - CODE 4187
- CODE 2628 - 20CY

A.F. GEOPHYSICS LABORATORY
L.G. HANSCOM FIELD
BEDFORD, MA 01730
- DR. T. ELKINS
- DR. W. SWIDER
- MRS. R. SAGALYN
- DR. J.M. FORBES
- DR. T.J. KENESHEA
- DR. J. AARONS
- DR. H. CARLSON
- DR. J. JASPERSE

CORNELL UNIVERSITY
ITHACA, NY 14850
- DR. W.E. SWARTZ
- DR. R. SUDAN
- DR. D. FARLEY
- DR. M. KELLEY

HARVARD UNIVERSITY
HARVARD SQUARE
CAMBRIDGE, MA 02138
- DR. M.B. McELROY
- DR. R. LINDZEN

INSTITUTE FOR DEFENSE ANALYSIS
400 ARMY/NAVY DRIVE
ARLINGTON, VA 22202
- DR. E. BAUER

MASSACHUSETTS INSTITUTE OF TECHNOLOGY
PLASMA FUSION CENTER
LIBRARY, NW16-262
CAMBRIDGE, MA 02139

NASA
GODDARD SPACE FLIGHT CENTER
GREENBELT, MD 20771
- DR. S. CHANDRA
- DR. K. MAEDA
- DR. R.F. BENSON

NATIONAL TECHNICAL INFORMATION CENTER
CAMERON STATION
ALEXANDRIA, VA 22314
- 12CY ATTN TC

COMMANDER
NAVAL AIR SYSTEMS COMMAND
DEPARTMENT OF THE NAVY
WASHINGTON, D.C. 20360
- DR. T. CZUBA

COMMANDER
NAVAL OCEAN SYSTEMS CENTER
SAN DIEGO. CA 92152
- MR. R. ROSE - CODE 5321

NOAA
DIRECTOR OF SPACE AND ENVIRONMENTAL LABORATORY
BOULDER, CO 80302
- DR. A. GLENN JEAN
- DR. G.W. ADAMS
- DR. D.N. ANDERSON
- DR. K. DAVIES
- DR. R. F. DONNELLY

OFFICE OF NAVAL RESEARCH
800 NORTH QUINCY STREET
ARLINGTON, VA 22217
- DR. G. JOINER

PENNSYLVANIA STATE UNIVERSITY
UNIVERSITY PARK, PA 16802
- DR. J.S. NISBET
- DR. P.R. ROHRBAUGH
- DR. L.A. CARPENTER
- DR. M. LEE
- DR. R. DIVANY
- DR. P. BENNETT
- DR. F. KLEVANS

PRINCETON UNIVERSITY
PLASMA PHYSICS LABORATORY
PRINCETON, NJ 08540
DR. F. PERKINS

SCIENCE APPLICATIONS, INC.
1150 PROSPECT PLAZA
LA JOLLA, CA 92037
DR. D.A. HAMLIN
DR. L. LINSON
DR. E. FRIEMAN

STANFORD UNIVERSITY
STANFORD, CA 94305
DR. P.M. BANKS

U.S. ARMY ABERDEEN RESEARCH
AND DEVELOPMENT CENTER
BALLISTIC RESEARCH LABORATORY
ABERDEEN, MD
DR. J. HEIMERL

UNIVERSITY OF CALIFORNIA,
BERKELEY
BERKELEY, CA 94720
DR. M. HUDSON

UNIVERSITY OF CALIFORNIA
LOS ALAMOS SCIENTIFIC LABORATORY
J-10, MS-664
LOS ALAMOS, NM 87545
M. PONGRATZ
D. SIMONS
G. BARASCH
L. DUNCAN
P. BERNHARDT

UNIVERSITY OF CALIFORNIA,
LOS ANGELES
405 HILLGARD AVENUE
LOS ANGELES, CA 90024
DR. F.V. CORONITI
DR. C. KENNEL
DR. A.Y. WONG

UNIVERSITY OF MARYLAND
COLLEGE PARK, MD 20740
DR. K. PAPADOPOULOS
DR. E. OTT

UNIVERSITY OF PITTSBURGH
PITTSBURGH, PA 15213
DR. N. ZABUSKY
DR. M. BIONDI
DR. E. OVERMAN

UTAH STATE UNIVERSITY
4TH AND 8TH STREETS
LOGAN, UTAH 84322
DR. R. HARRIS
DR. K. BAKER
DR. R. SCHUNK

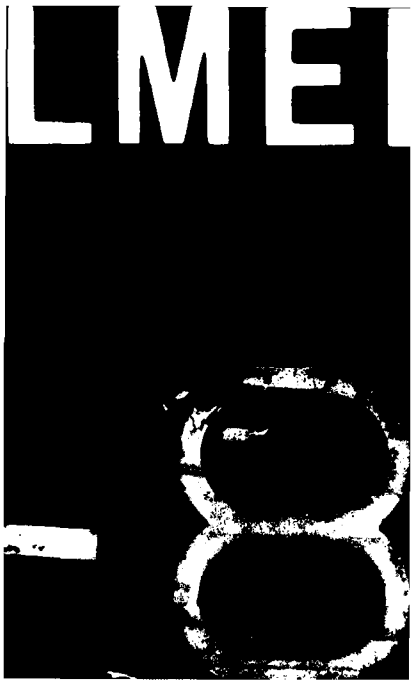
LME